Model for alpha particle induced nuclear reactions: ^{93}Nb(α,$x\alpha ypzn$) from 40–140 MeV

Ettore Gadioli and Enrica Gadioli-Erba
Dipartimento di Fisica dell'Università di Milano, Sezione di Milano, Italia
and Istituto Nazionale di Fisica Nucleare, Sezione di Milano, Italia

James J. Hogan
Department of Chemistry, McGill University, Montreal, Quebec, Canada
and Nuclear Science Division, Lawrence Berkeley Laboratory, Berkeley, California 94704

Barbara V. Jacak*
Department of Chemistry, University of California, Berkeley, California
and Nuclear Science Division, Lawrence Berkeley Laboratory, Berkeley, California 94704
(Received 19 January 1983)

A comprehensive model is introduced for alpha particle induced nuclear reactions. Five different mechanisms are examined and discussed. These include inelastic scattering of the incident alpha particle, nucleon pickup, binary fragmentation, dissolution of the alpha in the nuclear field, and preequilibrium processes initiated by alpha-nucleon collisions. A series of experiments was performed to measure the excitation functions of many nuclides produced from the irradiation of ^{93}Nb by 40–140 MeV alpha particles. Together with alpha particle and proton spectra measured by other authors, these data form the basis of a test of the model introduced. A detailed analysis of the comparison between the calculated and experimental results, with particular emphasis on the interpretation of breakup processes, leads to the conclusion that breakup to four nucleons is preferred to the more commonly assumed binary fragmentation in that a much broader range of experimental data may be reproduced.

[NUCLEAR REACTIONS ^{93}Nb(α,xn), $x=1-5$; (α,p6n), (α,2pxn), $x=1$, 5–7; (α,3pxn), $x=5-8$, 10; (α,4pxn), $x=5-7$, 9; (α,5p9n), (α,6p7n); ^{90}Zr, p spectrum; ^{93}Nb, p, and α spectra; $E=40-140$ MeV; introduced model; calculated: $d\sigma/dE_p$, $d\sigma/dE_\alpha$, $\sigma(E_\alpha)$ for all measured excitation functions.]

I. INTRODUCTION

During the last decade, phenomenological models for preequilibrium decay have proven to be highly successful in reproducing and predicting a wide range of charged particle spectra and excitation functions induced by protons of energy up to 200 MeV on target nuclei spanning the entire Periodic Table of the elements.[1–6]

Similar analyses of alpha particle induced reactions have produced less satisfactory results. Recent studies of Michel and Brinkmann,[7] Gallagher *et al.*,[8] and Ibowski *et al.*,[9] of the reactions induced by alpha particles of up to 170 MeV on targets of ^{59}Co, ^{103}Rh, and ^{232}Th indicate somewhat disappointing agreement between experiment and calculations based on hybrid models,[1] the quasifree scattering model,[10] and the modified exciton model.[11] Various reasons have been suggested for this disagreement including neglect of effects like fragmentation of the alpha particle and emission of preformed clusters from the target nucleus, or limitations on the number of particles emitted in the preequilibrium cascade.

The present work was motivated by the hope of gaining a better understanding of the mechanisms by which an alpha particle interacts with the nucleus. We present here the excitation functions of 29 reactions induced by 40–140 MeV α particles incident upon ^{93}Nb which were measured by activation techniques. These are compared with the calculated results of a new model, called OMEGA, which is described in detail. This model, based on approaches we have taken previously with the exciton model, considers five different types of interaction between the incident alpha and the target nucleus.

Reasonable reproduction of the excitation functions for spallation residues and of charged particle spectra has been obtained with this model. The predominant contributions to the total reaction cross section have been found to arise from mechanisms in which the alpha particle breaks up; however, the probability of survival of the alpha is far from negligible as demonstrated by the continuous spectrum of inelastically scattered alphas found experimentally, and reproduced by the theory.

After presenting the experimental procedure and results, and a detailed description of the OMEGA calculation, Sec. IV is devoted to a thorough examination of all the experimental data currently available. We will explore the implications of breakup to two, or four, fragments, and we will conclude that the proton spectra may be accounted for either by binary fragmentation or by our

model; however, the excitation functions measured in this work as well as the coincidence experiments of Koontz *et al.*[12] are found to be better reproduced assuming a breakup to four nucleons.

In the final sections of the discussion, we examine the different types of spallation excitation functions and relate them to the different fundamental interactions of the incident alpha particle and the target nucleus.

II. EXPERIMENTAL PROCEDURE AND RESULTS

Experiments at energies up to and including 100 MeV were carried out using the extracted beam of the 88-inch cyclotron of the Lawrence Berkeley Laboratory, at precisely determined bombarding energies. Those at the higher energies (140 and 120 MeV) were performed simultaneously at the University of Maryland Cyclotron, using an extracted 140 MeV alpha beam with copper degraders to reduce the beam energy to approximately 120 MeV. The total thickness of copper separating the two target foils was 454.9 mg/cm^2. The target foils and beam monitors were identical in both sets of irradiations. Targets were of nominally 0.025 mm high purity Nb metal foil, carefully weighed and cut to size to determine the average thickness.

The beam intensity was monitored by measurement of the cross sections of reactions induced in high purity nominally 0.025 mm Al foils placed downstream of the target in the Berkeley experiments and upstream of the first target foil in the Maryland experiments. The monitor cross sections were, above 60 MeV, that of the ^{27}Al(α,4p3n)^{24}Na reaction, and below 60 MeV that of the ^{27}Al(α,2p)^{29}Al reaction.[13]

The average beam energy incident upon a given foil, target, degrader, or monitor was calculated from the stopping power tables of Williamson and Boujot.[14] In this work, reference will be made to experiments at 40,60, . . . , 140 MeV, although the actual values of the incident energy, after all corrections are made for beam degradation, were calculated to be 39.0, 59.3, 79.2, 99.3, 119.7, and 139.1 MeV. Except for the 119.7 experiment, the uncertainty in the beam energy is less than 1.5 MeV; at 119.7 MeV, the uncertainty is $\pm$1.5 MeV.

After irradiation, the target and monitor foils were analyzed using gamma ray spectroscopy. Large volume Ge(Li) detectors (60—90 cm^3 active volume) were used in conjunction with 4000 channel pulse height analyzers to record spectra over a period of about two weeks. Gamma ray intensities were measured using standard peak fitting routines and the decay curves analyzed through least squares analysis. In Table I, the pertinent decay scheme data[15] used in this work for the measurement of the various spallation product residues are listed. Because of the existence of a large number of isomers, with quite short and quite long lifetimes, and in several cases more than one nuclide populating a given nuclear level, several of the decay curves, notably those of the $A=68$ and 87 mass chains, are quite complex and the estimated cross section for production of these nuclides depends quite sensitively on the relatively small errors in the adapted values of branching ratios, conversion coefficients, and isomeric transitions. For this reason, wherever it appeared feasible, more than one gamma ray was used to evaluate a given cross section; in the case of complex chains like those mentioned above, as many as four or five gamma rays, independently measured, contributed to a complete analysis of an isobaric chain.

The experimental results are presented in Table II.[16,17] The uncertainties reported arise from three sources only: statistical errors intrinsic to the peak height evaluation, uncertainties coming from the decay curve analysis, and discrepancies between independent measurements (different gamma rays) of a given nuclide.

They do not include systematic errors introduced from uncertainty in the beam monitoring, the parameters of the decay schemes, the efficiency curves for the several Ge(Li) detectors used, or from small effects such as recoil of products out of the target foils, or errors in the target mass and thickness. Except at 40 MeV, the beam monitor is thought to lead to an error on the estimated cross sections of not more than 2—3 %, the efficiency curves about 3—5 %, and other effects about 1%. The principal systematic error unquestionably arises from the decay schemes, particularly for those cases involving complex decay curves and isomers where evaluation of the conversion coefficients plays a major role. In these isolated cases, errors of as much as 30% may be introduced.

While this manuscript was being prepared we became aware of a similar set of experiments performed by Ernst *et al.*[18] using the stacked foil technique for up to 171 MeV alphas incident upon ^{93}Nb. Their experimental cross sections have been included in the figures where experimental data and theoretical calculations are compared. For the most part, except for a few cases which will be noted and discussed at suitable points in the discussion of the comparison between calculated and experimental results, the agreement between the two sets of experiments is reasonable, generally improving as the incident energy increases.[19,20]

III. THEORETICAL CALCULATIONS

In recent years, studies of the interaction of energetic alpha particles with complex nuclei have indicated that as many as five different mechanisms may be to some extent responsible for the experimentally observed results. To be reasonably complete, a theory must account for the yields, angular distributions, and energy spectra of charged particles, as well as for the excitation functions of several types of reactions like, e.g., the simple (α,2n) reaction occurring largely by preequilibrium or direct processes, and the very complex reactions characterized by large deposition energies, with many particles evaporated.

The five mechanisms often have no clear boundaries; however, it is clear from experimental data that a theory of alpha particle induced reactions must include: (1) inelastic scattering of the incident alpha particle by the target nucleus as a whole, leading to excitation of low lying collective states[21]; (2) pick-up reactions: creation of ^{5}He or ^{5}Li, followed by a breakup to a kinematically correlated alpha particle plus a nucleon[22]; (3) binary fragmentation of the alpha particle[12,20,23]; (4) dissolution of the alpha

TABLE I. Decay characteristics of nuclides studied.

Nuclide	Half-life	Gamma ray energy, keV	I_γ γ/decay	Comment
^{24}Na	15.0 h	1369	1.0	
^{29}Al	6.56 min	1273	0.892	
^{82}Rb^m	6.3 h	554.3	0.70	
^{83}Rb	83.0 d	520.4	0.47	
^{83}Sr	33.0 h	381.5	0.60	
^{84}Rb	33.0 d	881.5	0.734	
^{84}Y	38.5 min	795	0.95	complex
		975	0.72	
^{84}Zr	16.0 min	1040	0.55	via ^{84}Y
^{86}Y^m	48.0 min	208	0.94	
^{86}Y^g	14.6 h	627.7	0.325	
^{86}Zr	16.5 h	243	0.96	
^{87}Sr^m	2.8 h	388	0.80	
^{87}Y^m	12.7 h	381	0.74	complex
^{87}Y^g	80.3 h	484	0.92	complex
^{87}Zr	1.6 h			via ^{87}Y^{m,g}
^{88}Y	106.6 d	898	0.943	
		1836	0.993	
^{88}Zr	83.4 d	393.7	0.973	
^{88}Nb^m	7.8 min	1082	0.573	
		1057	0.90	
		399.4	0.426	
^{88}Nb^g	14.3 min	1082	0.979	
		1057	1.0	
		399.4	0.315	
^{89}Zr^g	78.4 h	909.2	0.99	
^{89}Nb^m	66.0 min	588	1.0	
^{89}Nb^g	2.03 h	588	0.93	
^{90}Y^m	14.6 h	1129	0.92	
^{90}Mo	5.67 h	257.3	0.776	
^{91}Y^m	49.7 min	555.6	0.949	
^{91}Mo	15.5 min	1637.3	1.0	
^{92}Nb^m	101.4 d	934	0.973	
^{92}Tc	4.4 min	329.3	0.78	
^{93}Mo^m	6.95 h	263	0.58	
		1477	0.983	
^{93}Tc^m	43.5 min	1363	0.80	via ^{93}Tc^g
^{93}Tc^g	2.75 h	1363	0.66	
^{94}Tc^m	52.5 min	871	0.94	
^{94}Tc^g	293.0 min	702.6	1.0	
		871	1.0	
^{95}Nb^m	90.0 h	235.7	0.975	
^{95}Nb^g	34.97 d	765.8	0.998	
^{95}Tc^m	60.0 d	204	0.662	
^{95}Tc^g	20.0 h	765.8	0.93	
^{96}Tc	4.35 d	778	0.991	

particle into four nucleons in the nuclear field[1,2]; (5) interaction of the alpha particle with individual nucleons of the target nucleus, leading to a preequilibrium cascade of alpha-nucleon scatterings; during this cascade the alpha particle may break up to four nucleons following any collision.[10,24]

There is obvious overlap between the last three processes in that each leads to the destruction of the alpha particle and the initiation of a preequilibrium cascade. Further, some authors may argue the fourth and fifth mechanisms may be in fact the same process, and the third merely a special case of either. Nevertheless, because in this work each leads to a definably different result of the alpha particle-target nucleus interaction, we retain for purposes of discussion the five mechanisms. For the sake of clarity where ambiguity may arise, "fragmentation" refers to process (3) producing two fragments, "dissolution" to process (4) in which the alpha energy is shared only between its four constituent nucleons, and "breakup" refers to process (5) initiated by the collision of the alpha

TABLE II. Cross section in mb for ^{93}Nb(α,x) measured experimentally.

			Beam energy, MeV					
A	Isomer	Nuclide	140	120	100	80	60	40
82	^{82}Rb^m		4.9 ±0.2	2.3±0.7				
83		^{83}Rb	2.6 ±0.3					
		^{83}Sr	12.9 ±1.9	5.8±1.0				
84		^{84}Rb	2.9 ±0.4	1.8±0.3				
		^{84}Y	7.3 ±0.4	5.8±0.3				
		^{84}Zr	1.5 ±0.3	0.9±0.2				
86	^{86}Y^m		64.9 ±2.8	27.7 ±2.1	12.4 ±0.4	10.4 ±0.3		
	^{86}Y^g		49.5 ±5.1	10.5 ±2.5	3.9 ±0.4	3.2 ±0.3		
		^{86}Y	114.4 ±5.8	38.2 ±3.3	16.3 ±0.6	13.6 ±0.5		
		^{86}Zr	46.7 ±1.8	14.3 ±0.9	1.4 ±0.1			
87	^{87}Sr^m		0.5 ±0.1	1.1 ± 0.5	2.0 ±1.0	0.38±0.16	0.58±0.45	
	^{87}Y^m		61.0 ±5.1	53.3 ± 2.6	23.1 ±0.6	8.0 ±0.3	4.28±0.18	
	^{87}Y^g		4.7 ±0.9	9.8 ± 1.9	3.3 ±0.2	0.24±0.02	0.26±0.02	
		^{87}Y	65.7 ±5.2	63.1 ±10.1	26.4 ±0.6	8.24±0.30	4.54±0.18	
		^{87}Zr	103.5 ±6.4	131.2 ± 9.2	60.7 ±2.2	3.08±0.38	1.18±0.21	
88		^{88}Y	41.9 ± 2.6	40.7 ± 1.8	27.5 ±1.4	6.9 ±1.8	4.6 ±0.06	
		^{88}Zr cum	194.0 ±19.0	144.0 ±16.0	173.0 ±5.0	37.0 ±1.0		
	^{88}Nb^m		6.5 ± 0.3	6.8 ± 0.3	2.4 ±0.2	1.3 ±0.7		
	^{88}Nb^g		35.4 ± 1.9	22.2 ± 0.8	30.2 ±1.4	3.0 ±0.3		
		^{88}Nb	42.1 ± 1.9	29.0 ± 0.9	32.6 ±1.5	4.3 ±0.8		
		^{88}Zr	153.9 ±19.1	115.0 ±16.1	140.4 ±5.3	32.7 ±1.3		
89		^{89}Zr cum	280.0 ±10.0	230.0 ±10.0	153.0 ±4.0	216.0 ±5.0	13.6 ±0.4	
	^{89}Nb^m		4.6 ± 0.3	3.5 ± 0.2	6.8 ±0.1	8.7 ±0.5	1.05±0.12	
	^{89}Nb^g		136.9 ±12.0	124.2 ± 9.1	47.9 ±2.8	72.5 ±3.1	<1	
		^{89}Nb	141.5 ±12.1	127.7 ± 9.2	54.7 ±2.8	81.2 ±3.1	<2.0 ±1.0	
		^{89}Zr	138.5 ±15.3	102.3 ±16.9	98.3 ±5.0	134.8 ±5.8	11.6 ±1.5	
90	^{90}Y^m				1.5 ±0.1	0.97±0.90		
		^{90}Nb	192 ±16	254 ±24	211 ±5	81.9 ±1.4	194.0 ±3.0	
		^{90}Mo	55 ±6	90 ±5	63 ±2	1.87±0.28		
91	^{91}Y^m		0.40±0.22	0.78±0.11	0.52±0.05	0.25±0.04		
92	^{92}Nb^m		39.0 ±1.6	40.2 ±1.7	36.1 ±0.9	33.8 ±0.9	36.1 ±0.9	18.3 ±0.5
		^{92}Tc	9.3 ±0.4	18.0 ±0.6	23.8 ±2.8	75.7 ±3.6	46.0 ±0.2	
93	^{93}Mo^m		3.76±0.24	7.65±0.45	6.59±0.11	14.1 ±2.1	91 ±2	2.01± 0.05
	^{93}Tc^m		1.45±0.9	2.82±0.19	3.93±0.72	14.7 ±1.6	55 ±10	1.81± 0.40
	^{93}Tc^g		35.1 ±1.4	59.9 ±8.1	67.9 ±2.	121 ±3.	376 ±12	2.6 ± 0.2
		^{93}Tc	36.55±1.4	62.72±8.1	71.83±2.	135.7 ±3.	431 ±12	4.41± 2.1
94	^{94}Tc^m		0.57±0.31	0.78±0.04	1.20±0.07	2.94±0.18	10.3 ±0.5	92.3 ± 3.8
	^{94}Tc^g		5.0 ±0.3	11.6 ±0.6	16.6 ±0.3	39.5 ±0.7	145 ±24	931 ±17
		^{94}Tc	5.6 ±0.5	12.4 ±0.7	17.8 ±0.3	42.4 ±0.8	155 ±24	1023 ±18
95	^{95}Nb^m				0.46±0.06	0.73±0.11	1.19±0.15	1.06±0.10
	^{95}Nb^g				0.09±0.02	0.10±0.02	0.11±0.02	0.14±0.03
		^{95}Nb			0.55±0.07	0.83±0.12	1.30±0.16	1.20±0.11
	^{95}Tc^m					1.3 ±0.2	3.4 ±0.2	14.4 ±0.4
	^{95}Tc^g				4.96±0.27	12.9 ±0.4	38.9 ±0.5	213 ±2
		^{95}Tc			4.96±0.27	14.2 ±0.5	42.3 ±0.5	227 ±3
96		^{96}Tc			0.49±0.02	1.21±0.02	3.8 ±0.1	11.5 ±0.2

with an individual nucleon.

The first two mechanisms contribute chiefly to the charged particle spectra, particularly for alpha particles, while affecting the pattern of spallation product excitation functions only for very simple reactions like (α,α) $(\alpha,\alpha n)$, and $(\alpha,\alpha p)$. The last three mechanisms, all leading to preequilibrium cascades, are the basis of nearly all the spallation results and the soft, isotropic, evaporation components of the charged particle spectra, and contribute a large fraction of the higher energy, forward peaked, components of the spectra. Thus, this work deals mainly with the last three mechanisms.

The calculation described below in detail, in which we consider all five mechanisms, has been named OMEGA. The following describes the treatment of the five mechanisms, as well as other facets of the theory.

A. Inelastic scattering of the alpha particle with the nucleus as a whole

The highest energy part of the alpha particle spectrum, at the forward angles, shows that discrete levels of the residual nucleus in (α,α') reactions are excited. These have usually been attributed to inelastic scattering of the alpha particle exciting low lying collective levels. This high energy region usually extends to a broad peak corresponding to excitation of the isoscalar quadrupole resonance[21] which in the case of ^{93}Nb is at about 14 MeV. This mechanism comprises at most a few percent of the total reaction cross section. For purposes of this work, no attempt was made to evaluate the probability of inelastic scatterings leading to discrete states. Rather the following assumption was made: Inelastic scatterings lead to the formation of ^{93}Nb, excited to all energies up to that of the isoscalar giant quadrupole resonance (IGQR), with equal probability, i.e., with a uniform distribution of excitation energy from 0 to 14 MeV. Further, the nucleus is allowed to undergo evaporation in the usual fashion.

B. Pick-up reactions: ^{5}He and ^{5}Li

At the extreme forward angles of the (α,α') energy spectrum, Chevenert *et al.*[22] interpreted their experiment data as arising from the breakup of ^{5}He (or ^{5}Li) formed in pickup reactions. Subsequent coincidence measurements of Brown *et al.*[25] on kinematically correlated α + neutron pairs have confirmed this mechanism and allowed an evaluation of its magnitude. (Owing to the effect of the Coulomb barrier, the analogous pickup of a proton producing ^{5}Li is expected to have a much smaller cross section.) From these kinematic studies of the coincidence data, it may be concluded that the residual nucleus to a large extent plays a spectator role in these interactions, being excited only to low energy. Brown *et al.*[25] have found the pickup mechanism producing ^{5}He to account for $\sim$30 mb of cross section for an alpha energy of about 90 MeV on heavy nuclei. The total reaction cross section for ^{93}Nb is greater than 1500 mb; thus production and breakup of ^{5}He accounts for $\sim$2% of all events and contributes only to the $(\alpha,\alpha n)$, and to a small extent to the $(\alpha,\alpha p)$ spallation reactions. Since neither of these reactions was measured in this work, this mechanism is ignored in the OMEGA code. These first two of the five mechanisms taken together comprise about 5% of alpha particle-target nucleus interactions; they are discussed in Ref. 24, and are not treated further in this work.

C. Binary fragmentation

The third mode of interaction between the alpha particle and the target nucleus mainly leads to emission of a fragment of the alpha at forward angles with a velocity corresponding to that of the incident beam. Holmgren and co-workers[12,20,23] interpreted this result as suggesting a fragmentation of the alpha into two pieces in a peripheral interaction with the nucleus. Studies of fast particle-fast/slow particle coincidences, specifically of the energy distribution of emitted particles, concluded that the complement of the observed fragment is most likely absorbed by the target nucleus; the resultant excited system undergoes deexcitation partly by the preequilibrium cascade, but mainly by evaporation.[12,23]

There are three possible modes of binary fragmentation of an α, to n + ^{3}He, p + t, and d + d. The energy distributions of d, t, and ^{3}He were found[20,23] to be approximately Gaussian in shape, with a mean centered about the beam velocity, and a variance which increases with increasing beam energy. In this work, the yields of d, t, and ^{3}He have been estimated from these studies of the Maryland group[20,23] on 80 and 160 MeV α incident upon ^{90}Zr. These have been assumed to be the signature of a binary fragmentation process. Simple linear interpolation of the experimental data was used to determine the relative probability and the energy distribution of particles emitted in these fragmentation processes at other incident energies.

A determination of the yields of the three binary fragmentation processes according to the procedure described above suggests that the events leading to emission of one fast particle with essentially beam velocity in the forward direction with absorption of the complementary fragment comprise a minor fraction, of the order of 10%, of the reaction cross section. This is a different interpretation of the same experimental data than that concluded by Holmgren and co-workers[12,20,23] who based their estimate of the fragmentation process on the yield of high energy protons. We return to these differing interpretations in Sec. IV A.

D. Dissolution of the alpha particle to four nucleons, in the nuclear field

This process occurs most likely at the nuclear surface. The assumption has been made that the alpha energy may be divided among the four nucleons with equal probability in all possible ways, in analogy with the equiprobability hypotheses of earlier exciton model studies.[1-3] The dissolution of the alpha particle originates a preequilibrium cascade of nucleon-nucleon interactions. In order to evaluate the absolute cross section of this reaction mechanism, the spectrum of highest energy protons is calculated and normalized to that measured. In fact, it should be noted that this mechanism is, in these calculations, the

primary source of the protons observed experimentally to have essentially the full beam energy.

Estimates of the cross section for this process have come from studies of 42 and 54.8 MeV α's incident upon ^{93}Nb (Refs. 27 and 28) and 140 MeV α's on ^{90}Zr.[26] It is found that this process accounts for about 500 mb of cross section at $E_\alpha \approx 50$ MeV, decreasing to 250 mb at 140 MeV. This energy dependence is consistent with a simple picture of the interaction. The impulse acting on the alpha is the product of the gradient of the nuclear potential times the interaction time of the alpha with the nucleus. The nuclear potential is relatively independent of the alpha energy. The interaction time, however, is proportional to $1/v$ and therefore to $E^{-1/2}$, roughly in keeping with the observed decrease. The cross sections for the dissolution of an alpha particle to four nucleons, at the other considered incident energies, was estimated by simple linear interpolation.

E. Alpha-nucleon collisions

This mechanism, including both multiple alpha scatterings and events in which the alpha breaks up to four nucleons, constitutes 60—70% of the total reaction cross section. Following interaction of the alpha particle with an individual nucleon of the target nucleus, one of three things may occur: (a) the alpha particle may be reemitted to the continuum; (b) the alpha may break up to four nucleons; (c) the alpha particle may undergo further scatterings with other nucleons in the nucleus. All three possibilities are considered.

The spectrum of alpha particle energies following collision with a nucleon has been evaluated from alpha-free nucleon scattering dynamics, details of which have been published.[24] Briefly, a nucleon is randomly selected from a Fermi momentum distribution, and the final state configuration is determined using free particle interaction cross sections. The Pauli exclusion principle is invoked to forbid those collisions leaving either particle with an energy less than its Fermi energy since no such final states are available. This configuration is then used as the initial state for an otherwise conventional preequilibrium exciton model calculation.

Emission of the alpha to the continuum is evaluated as is customary from consideration of phase space and inverse cross sections. Specifically, the decay rate for emission to the continuum following the ith collision, $W_C^{i,\alpha}(E,\epsilon_\alpha)d\epsilon_\alpha$, is assumed[24] to be, in analogy to emission rates for nucleons evaluated in the exciton model,[2,3]

$$W_C^{i,\alpha}(E,\epsilon_\alpha)d\epsilon_\alpha = \frac{1}{\pi^2\hbar^3}\mu_\alpha\epsilon_\alpha\sigma_{\text{inv}}(\epsilon_\alpha)\frac{P_i(\epsilon,\epsilon_\alpha)}{g_\alpha}d\epsilon_\alpha ,$$

where E is the excitation energy of the emitting nucleus; ϵ_α is the kinetic energy in the continuum of the alpha; μ_α is the reduced mass of the system; σ_{inv} is the inverse cross section taken from the optical model; $P_i(\epsilon,\epsilon_\alpha)$ is the spectrum, normalized to unity, of α particles, following the ith collision. The initial alpha energy, ϵ, is measured from the bottom of the well, and g_α is the alpha particle state density, from Ref. 24.

If the alpha particle is not emitted from the nucleus following the ith collision, it may either breakup or undergo further scattering. These two processes, being complementary, are evaluated simultaneously.

The total decay rate, $W_{\text{tot}}^{i,\alpha}(E)$, for further alpha-nucleon collisions has been evaluated using the imaginary part of the α optical potential. This total decay rate includes both scattering and breakup, and is given by

$$W_{\text{tot}}^{i,\alpha}(E) = \int P_i(\epsilon,\epsilon_\alpha)v\rho\bar{\sigma}_{\alpha\text{N}}(\epsilon_\alpha)d\epsilon_\alpha$$

taken to be approximately

$$W_{\text{tot}}^{i,\alpha}(E) \approx \frac{2}{\hbar}\int P_i(\epsilon,\epsilon_\alpha)W_{\text{opt}}(\epsilon_\alpha)d\epsilon_\alpha ,$$

where $W_{\text{opt}}(\epsilon_\alpha)$ is the depth of the imaginary part of the optical potential for an alpha with energy ϵ_α,[29,30] v is the velocity of the alpha, ρ is the nuclear density, $\bar{\sigma}_{\alpha\text{N}}$ is the average alpha-nucleon scattering cross section in nuclear matter, and $P_i(\epsilon,\epsilon_\alpha)$ is defined above.

In previous work, the probability of breakup was usually taken to be a free parameter.[10,24]

In this work, we have explicitly defined the breakup probability as a function of energy. We make the following evaluation:

$$W_{\text{tot}}^{i,\alpha}(E) = W_{\text{bu}}^{i,\alpha}(E) + W_{\text{s}}^{i,\alpha}(E) ,$$

where W_{bu} and W_{s} are the breakup and scattering decay rates, respectively. Further,

$$W_{\text{bu}}^{i,\alpha}(E) = kW_{\text{s}}^{i,\alpha}(E) ,$$

the ratio, k, is evaluated explicitly as

$$k = \frac{\sigma_{\text{inelastic}\,\alpha\text{N}}}{\sigma_{\text{elastic}\,\alpha\text{N}}} ,$$

where $\sigma_{\text{inelastic}\,\alpha\text{N}}$ and $\sigma_{\text{elastic}\,\alpha\text{N}}$ are the inelastic and elastic α-nucleon scattering cross sections evaluated for that relative center of mass energy in free space which is equal to the average energy of the alpha-nucleon pair in nuclear matter. Thus the assumption introduced in this work is that an α particle interacting with a nucleon in the nucleus, at a given center of mass energy, has the same probability of undergoing inelastic scattering, i.e., breakup as it would if the interaction had occurred in free space. In practice, in the OMEGA calculation, k is evaluated for an alpha-nucleon relative energy averaged over the nucleon momentum distribution. During the calculation of scattering or breakup probability, other possible modes of decay of the composite system are ignored. (See below, Sec. III G.)

In the series of equations above for the various decay rates, the only quantity remaining to be evaluated is the energy spectrum of alphas following the ith collision. This is determined by a folding procedure.

The energy spectrum of alpha particles following a single collision, $P_1(\epsilon'_\alpha,\epsilon_\alpha)$, is, as stated above, calculated from alpha-nucleon free scattering kinematics. The shape of the spectrum following collisions subsequent to the first is generated by

$$P_i(\epsilon,\epsilon_\alpha) = \int P_{i-1}(\epsilon,\epsilon'_\alpha)P_1(\epsilon'_\alpha,\epsilon_\alpha)d\epsilon'_\alpha .$$

This concludes a discussion of the quantities necessary

to evaluate the probability of occurrence of each of the three most probable decay modes after the interaction of the alpha with a nucleon in the target nucleus. Evaluation of these three decay rates allows the tracing of the preequilibrium cascade. While the results of this approach are discussed in detail in Sec. IV, it is worth summarizing the preequilbrium calculation in concise form since processes initiated by an alpha-nucleon collision constitute 60—70 % of the total reaction cross section. Of such processes, about 60—75 % of the time the alpha particle will eventually break up with the percentage slowly increasing over the energy range from 40—140 MeV. The probability of alpha reemission again increases with increasing incident energy from 10% to 25% of the events beginning with an alpha-nucleon collision. The probability of the alpha undergoing multiple scatterings without breakup or emission, until its energy is smaller than the Coulomb barrier, decreases from the order of 30% at the lowest energies, to less than 5% at the highest.

Overall, the five mechanisms described above contribute to the total reaction cross section for 40 to 140 MeV α's on ^{93}Nb approximately as follows: (1) inelastic scattering ($\sim$5% at all energies); (2) pickup reactions ($\sim$2% at all energies); (3) binary fragmentation ($\sim$10% at all energies); (4) dissolution in the nuclear field (decreasing with energy from 30% to 15%); (5) alpha-nucleon collisions (reemission of alpha increases with energy from 5% to 20%, breakup of alpha increases with energy from 35% to 50%, multiple scattering only decreases with energy from 15% to 0%).

F. Evaporation: Angular momentum effects

In this work, we considered the effect of angular momentum imparted to the nucleus, during the preequilibrium cascade, on the evaporation of particles from the excited composite nucleus. Although the procedure adopted is a simplified one, it is clearly an improvement on our earlier works[2–6] in which the angular momentum of the decaying system played no role.

During the preequilibrium cascade, it is assumed that the angular momentum of a particle emitted either in a first chance preequilibrium event, or following the dissolution, fragmentation, or breakup of the alpha particle, is completely aligned with that of the incident particle. The resulting value of the angular momentum of the residual system is the difference between the incident and emitted particle angular momenta. The assumption of perfect alignment somewhat overestimates the average angular momentum removed by the emitted particle. To partially compensate for the error thus introduced, the assumption is made that a second preequilibrium emission does not affect the angular momentum of the excited nucleus.

When the system reaches equilibrium, its rotational energy is calculated using the rigid body moment of inertia. The assumption is then made that particle evaporation is forbidden if the excitation energy of the emitting nucleus is less than the sum of the binding energy, Coulomb energy, and nuclear rotational energy. Thus evaporation is forbidden to states of the residual nucleus which lie below the yrast level.

If serious errors were introduced by this highly approximate procedure, they would likely result in poor reproduction of the excitation functions near the threshold where evaporation from a compound nucleus is the chief mechanism of production. Such a systematic error does not in fact exist so the approximations would seem to be justified *a posteriori* and should not affect the mechanistic conclusions we reach for the wide range of reactions studied in this work.

G. Procedure of the calculation

Of the five mechanisms for the interaction of an alpha particle and a target nucleus listed above, the last three lead to preequilibrium cascades each having a different initial configuration. Binary fragmentation, as we have used the term in this work, leads to two fragments, one of which is absorbed by the target nucleus. For example, fragmentation to p and t, followed by absorption of the triton leads to a cascade whose initial configuration is 3 particle-0 hole, with an excitation energy distribution which is roughly Gaussian and centered about three-fourths of the beam energy. In the discussion of the alternative interpretations of the experimental charged particle spectra and coincidence data in Sec. IV, we examine the consequences of this starting configuration on the agreement between theory and experiment, particularly for the (α,2n) excitation function.

Dissolution of the alpha particle into four nucleons in the nuclear field produces an initial configuration of 4p0h with the beam energy (corrected for the Q value and center of mass motion) converted to excitation energy.

Collision processes between the incident alpha and a nucleon of the target nucleus lead to initial configurations of 1α1p1h if the alpha survives collision or 5p1h if breakup has occurred.

Once one alpha particle is emitted during the preequilibrium phase, subsequent emission is assumed to occur by evaporation. If the alpha is emitted after only one or two scatterings, it retains most of its initial energy; the residual nucleus is excited to relatively low energy. If, on the other hand, the alpha is emitted after many scatterings, the residual nucleus has its energy distributed among many particles and holes. In neither case is it likely that further preequilibrium emission occurs.

During the cascades which follow the breakup of the alpha particle into its constituent nucleons, the possibility of interaction with performed alpha clusters in the nucleus is allowed, just as in our earlier exciton model calculations,[3,31,32] and with the same preformation constant.[32] The only process not considered is one in which the incident alpha encounters a preformed alpha cluster. Such a process is unlikely to be more than a minor contribution to the overall reaction cross section.

In computing the relative probabilities of α emission, α-nucleon scattering, or breakup, at any stage of the calculation, the decay modes of the composite system relating to the struck nucleon are ignored. These include the decay rate for emission to the continuum and for nucleon-nucleon interactions. In fact, the nucleon acquires a quite small energy; consequently, its emission rate

is small and the Pauli principle contributes to its low interaction rate. None of these approximations, which greatly simplify the calculation and reduce computation time, affect the results in any appreciable way.

At each energy, approximately 20 000 cascades were run giving a practical limit to the excitation function calculation of 0.1 mb with a 100% error. The other input data of the calculation (binding energies, level densities, pairing energies, etc.) are identical to those used in the earlier exciton model calculations. For complete listings and discussion, see Ref. 3.

IV. DISCUSSION

A. Breakup and fragmentation processes

Before proceeding to a comparison of the results of the OMEGA calculation with experiment, it is worth examining the model we present, and specifically, considering its interpretation of processes involving the breakup of the incident alpha particle. Our model leads to an interpretation different from that of Holmgren *et al.*[12,20,23] of the mechanism of alpha-nucleus interaction. Specifically it is felt that their experimental results do not necessarily imply that the major part of the proton yield (the dominant component of the fragment yields) is due to a process of binary fragmentation. Rather, as suggested above (Sec. III C), and in agreement with the calculations of Baur *et al.*,[33–36] the yields of d, t, and ^{3}He were taken as representative of binary fragmentation while we assumed the bulk of the proton yield arises from processes in which the alpha breaks up to four nucleons.

We will compare the two approaches while considering three specific experimental results strongly dependent upon the mode of breakup of the alpha particle. These include (1) the angle inclusive proton spectra, (2) the excitation functions of the "simple" reactions, e.g., (α,xn) of which the $(\alpha,2n)$ is discussed in detail below, and (3) the charged particle coincidence studies of Koontz *et al.*[12] not previously discussed in detail in this work.

1. *Proton spectra*

Experimentally, it was found[20–23] that, at forward angles, the proton spectrum shows a broad peak centered about one-quarter of the incident alpha energy. This result was interpreted as suggesting a two body breakup process; however, if one considers the breakup of the α into four nucleons, and invokes the equiprobability hypothesis discussed above (Sec. III D), the energy distribution of the proton emitted just after the breakup may be directly evaluated. Accounting for the availability of states, inverse cross sections, and phase space, the spectrum takes the shape of the product $U^2\epsilon\sigma_{\text{inv}}(\epsilon)$, where U is the excitation energy of the residual nucleus, and ϵ is the proton energy. Neglecting the energy dependence of the inverse cross section, this spectrum peaks at an energy one-third the maximum possible proton energy. Taking account of Q values, for incident α energies of 80 and 160 MeV on ^{90}Zr, the peaks occur at 23.4 and 48.9 MeV, respectively; however, at these energies, emissions occurring later in the cascade cannot be ignored. Since the exciton configuration is moving toward equilibrium, later emission tends to reduce further the energy at which the proton spectrum peaks.

Although angles are not considered explicitly in the OMEGA calculation, it is clear that emissions coming later in the cascade have lower average energies and larger angles with respect to the beam direction. This is in keeping with the experimental results.[20,23] Therefore, it is felt that while a process of binary fragmentation can be used to explain the features of the proton spectrum, the experimental data currently available do not rule out an alternative interpretation. A more complete discussion of the proton spectra calculated in this work appears in Sec. IV B.

2. *The $(\alpha,2n)$ excitation function*

If, in a binary fragmentation process, a neutron carries away about a quarter of the total available energy, the residual nucleus is left in a simple configuration with considerable excitation energy. There is then a substantial probability of emission of a second fast neutron, i.e., a non-negligible probability of deexcitation by a $(\alpha,2n)$ reaction. Note that, at 160 MeV, the emission of two fast neutrons is the only reasonable mechanism for $(\alpha,2n)$; any evaporation removing relatively low energy particles will almost certainly lead to emission of more than two particles. A calculation has been made of the contribution to the cross section of the processes in which the first neutron is emitted in a binary fragmentation, and the second during the intranuclear cascade following absorption of the complementary ^{3}He by the target nucleus, assuming that the total yield for binary fragmentation to a neutron is equal to that for a proton, taken from data of Wu *et al.*[20] for 80 and 160 MeV alphas incident upon ^{90}Zr. Simple linear extrapolation was used between the energy extremes. Making a different assumption, one with a rapidly increasing probability of breakup to a saturation value at energies near 160 MeV, leads to larger cross sections than those calculated below.

The energy distributions of the neutron fragment were taken to be identical to those of protons measured at 80 and 160 MeV, except for Coulomb barrier effects, again with linear interpolation of the mean and variance of the Gaussian shape between energies.

The results obtained from this calculation using both a 3p0h $(2\pi1\nu)$ (line 1) and 4p1h initial configuration properly weighted as to protons and neutrons (line 2) are compared in Fig. 1 with the experimental results[18,37,38] and the results of the OMEGA calculation. Presumably a more realistic estimate of this contribution would be somewhere between the two extremes. Taking into account that contributions from other alpha-nucleus interactions have not been included, this comparison shows that assuming a cross section for binary fragmentation of the magnitude of that estimated by Holmgren *et al.* would lead, at high incident energies, to noticeably poorer agreement with the experimental $(\alpha,2n)$ excitation function than that calculated in this work. Analogous results have been found to hold for the ^{59}Co$(\alpha,2n)$ reaction.

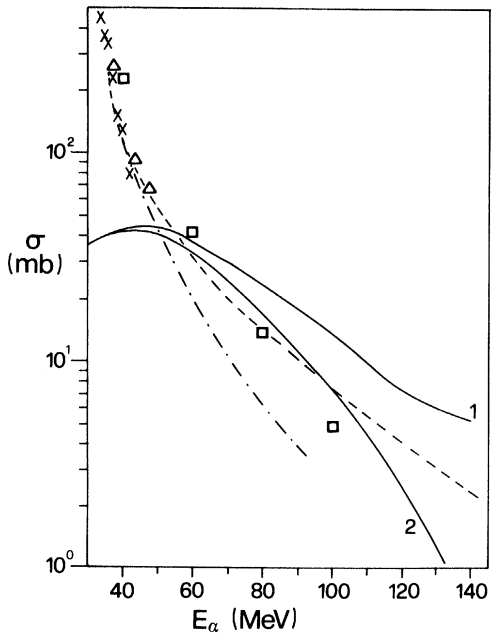

FIG. 1. Excitation function of the ^{93}Nb(α,2n)^{95}Tc reaction. Data points are from this work □; ×, Ref. 37; △, Ref. 38; ·—·, Ref. 18. The dashed line is the result of the OMEGA calculation. Lines 1 and 2 have been calculated in the hypothesis of binary fragmentation of the alpha with the assumptions discussed in the text.

3. *Coincidence measurements*

A coincidence study on the interaction of 140 MeV α's with ^{90}Zr by Koontz *et al.*[12] revealed that in coincidence with a fast proton at a given forward angle, the predominant charged particles are protons and alphas of "low energy" ($E < 20$ MeV) strongly peaked at small angles with the beam axis. The preponderance of fast particle-slow particle coincidences relative to fast particle-fast particle, and the forward angle peaking of coincident, mainly slow, particles, form the basis of a test of the consequences of the various modes of breakup of the alpha particle.

The first attempt to fit the data was made using the mechanism of "absorptive fragmentation" (called binary fragmentation with absorption of one fragment in this work and Refs. 12, 20, and 23) which is suggested to provide a reasonable explanation of the data. The fast proton energy spectrum was taken from Ref. 20. This served to define the excitation energy distribution of the composite nucleus after absorption of the complementary triton. A standard preequilibrium-evaporation calculation was then performed to specifically evaluate the multiplicity of slow ($E < 20$ MeV) and fast ($E > 20$ MeV) particles emitted in coincidence with the fast proton.

A calculation from a starting configuration of 3p0h ($1\pi 2\nu$) yielded the following multiplicities: from evaporation of protons plus alphas, 0.48 particles/event; from preequilibrium processes, fast protons, 0.40, and slow protons, 0.17. Overall, the ratio of slow to fast charged particle emission in coincidence with a fast proton is $(0.48 + 0.17)/0.40 = 1.6$. One must, however, take into account that the fast protons from the preequilibrium cascade following t absorption are predominantly concentrated within a relatively small cone concentrated about the triton direction, while the slow particles, and certainly those coming from evaporation, are not expected to be as highly correlated with the fast proton. Thus it may be concluded that *in the forward direction,* fast-fast coincidences should predominate over fast-slow ones. These results are in clear disagreement with the experimental data.

The disagreement is reduced if absorption of the triton is assumed to take place in conjunction with one interaction with a nucleon. This creates a 4p1h initial configuration, properly weighted as to protons and neutrons. Since the excitation energy is divided among more excitons, the incidence of fast particle emission is thereby reduced. The multiplicities calculated are the following: evaporation, 0.74; preequilibrium decay, 0.23 fast protons and 0.18 slow protons. Overall, the ratio of slow to fast particles is $(0.74 + 0.18):0.23 = 4$. However, as in the previous case, secondary fast particles are still strongly correlated with the primary proton and *in the forward direction,* the number of fast-fast coincidences is expected to be of the order of fast-slow ones.

A calculation was then performed using the alternative interpretation of the alpha-nucleus interaction proposed in this work. In this case, the calculation was "gated" on events in which there was a first chance preequilibrium emission of a proton and the multiplicities of *subsequent* preequilibrium and evaporative emission of charged particles evaluated. In this case, the results were as follows: slow protons (from preequilibrium plus evaporation), $0.040 + 1.085 = 1.125$; fast protons (from preequilibrium plus evaporation), $0.0367 + 0.0095 = 0.0462$. The ratio of slow to fast coincidences is greater than 24. This value is, in fact, a lower limit; evaporated alphas, a small, but nonnegligible component, were not included. It is clear from these numbers that even if one allows a more forward peaking of the secondary fast particles, the fast proton-slow charged particle coincidences will always predominate over fast-fast coincidences in keeping with the experimental data.[12]

The OMEGA calculation also accounts for the predominance of coincidences occurring between the fast proton and slow charged particles in the forward direction. The predominance of emission of slow particles in this direction is expected to arise from the mismatch between the high angular momentum of the incident α, $\vec{l}_\alpha$, and the low angular momentum of most of the emitted particles (mainly nucleons of energy considerably lower than that of the α). As a consequence it is estimated that the last evaporated particles should have an angular momentum considerably aligned to $\vec{l}_\alpha$ (Ref. 39) and they will be emitted isotropically in a plane perpendicular to $\vec{l}_\alpha$. Since $\vec{l}_\alpha$ can be rotated about the beam direction, the only outgoing particle directions common to all the planes are forward and backward with respect to the incident α direction. Then, we estimate that the fast preequilibrium particles and approximately one-half of the last evaporated particles will be concentrated in the forward cone. A detailed

calculation more approximate than those cited above suggests that the average number of coincident particles in the forward cone (corresponding to one steradian) would be about three times greater than coincidences out of this cone, in qualitative agreement with experimental findings.

B. Comparison of calculated results with experiment

The comparison of the results calculated using the OMEGA model described above with experimental results of several authors, including those of this work, is divided into five parts. These are the following: (a) alpha particle spectra; (b) proton spectra; (c) simple reactions, e.g., (α,xn); (d) alpha emission reactions, e.g., $(\alpha,\alpha xn)$; (e) complex reactions, e.g., $(\alpha,x\alpha ypzn)$. Specific examples of each are treated below.

1. Particle Spectra

a. Alpha particle spectrum: $^{93}Nb(\alpha,\alpha'X)$ at 54.8 MeV (Fig. 2). This spectrum, which has been analyzed in Ref. 24 is included here for completeness. The experimental work is that of Chevarier.[28] The spectrum was measured only for angles greater than 30°; hence it is unlikely that pickup processes involving ^{5}He or ^{5}Li contribute appreciably; however, two major, and several minor, components comprise the angle integrated spectrum.

The dominant process in the alpha particle spectrum of Fig. 2 is seen to be alpha emission following collision with one to four nucleons (full lines 1 to 4). The line labeled $\sum$ is the sum of all such interactions in which the alpha is reemitted to the continuum following one or more scatterings. A small peak in the experimental data, labeled IGQR, indicates excitation of the isoscalar giant quadrupole resonance. In the calculation of this spectrum, this mechanism was ignored; however, excitation of this mode was later included, as described above, in the OMEGA calculations of the excitation functions. For further discussion concerning the preequilibrium portion of the spectrum and the calculation of alpha particle angular distributions, see Ref. 24.

The dashed line at low energies arises principally from evaporation of alphas from equilibrated nuclei with a small additional component of preequilibrium emission of alpha clusters. Evaporation is somewhat overestimated with consequences observable in some of the excitation functions. These will be noted below.

b. Proton spectra: $^{93}Nb(\alpha,pX\cdots)$ at 42 and 54.8 MeV and $^{90}Zr(\alpha,pX\cdots)$ at 140 MeV. The experimental angle integrated proton spectra measured by West,[27] Chevarier *et al.*,[28] and Wu *et al.*[26] are compared with the calculated preequilibrium component, forseen by the OMEGA model, in Fig. 3. There are three major contributions to each calculated spectrum which fit the experimental data extremely well.

The first is from dissolution of the alpha particle to four nucleons in the nuclear field. This mechanism coupled with the assumption of equiprobability of population of available final states controls both the magnitude and the shape of the high energy portion of the specturm.

The other two components result from interactions of the alpha with individual nucleons. Either a struck proton may be directly emitted, or, following one or more collisions the alpha may breakup with subsequent proton emission. This mechanism, described in Sec. III E, contributes chiefly to the intermediate and lower energy regions of the spectra.

2. Spallation excitation functions

Before proceeding to a study of individual reactions, it is worth considering the overall picture of spallation events. As previously indicated, roughly 60—70% of the total cross section at all energies arises from events involving the collision of the incident α with individual nucleons. The cross section of this process is indicated by σ_R^α. In Fig. 4 the percentages of different processes which comprise σ_R^α are portrayed. In some cases, the incident alpha is reemitted after one or more collisions with nucleons. This process is labeled α,α'. Lines 1—5 indicate

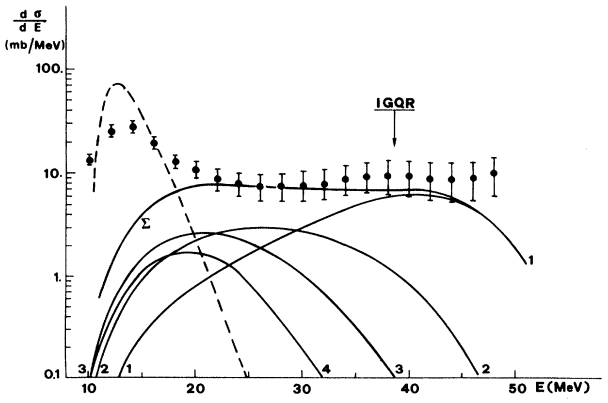

FIG. 2. The spectrum of alpha particles emitted in the ^{93}Nb$(\alpha,\alpha'X\cdots)$ reaction at 54.8 MeV. The experimental data, ●, are from Ref. 28. The full and dashed lines are the results of calculations (see text).

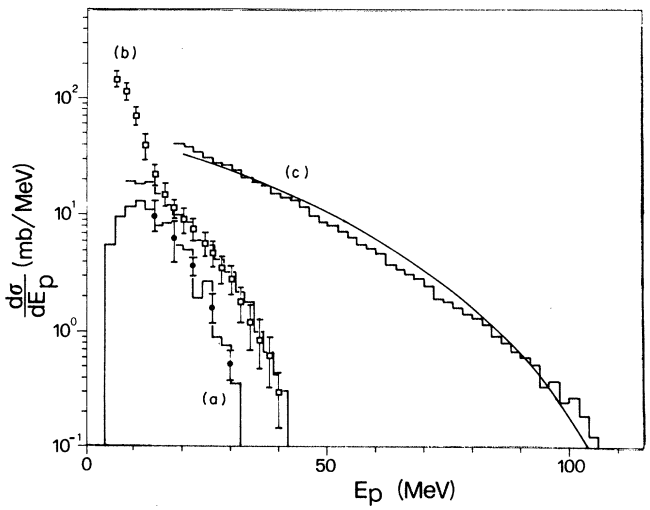

FIG. 3. Comparison of experimental proton spectra from α bombardment of ^{93}Nb at 42 MeV (Ref. 27) and 54.8 MeV (Ref. 28), respectively, (a) and (b), and ^{90}Zr at 140 MeV (Ref. 26), (c), full line, with the results of theoretical calculations, histograms.

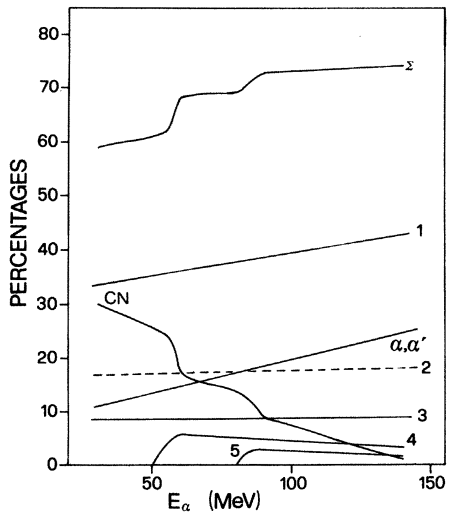

FIG. 4. The percentages of the various mechanisms which comprise σ_R^α (see text) are shown as a function of the incident alpha energy. The various lines are defined in the text.

events in which the alpha particle breaks up to four particles following 1—5 scatterings with nucleons. The line $\sum$ represents the summation of all such processes. Finally, if the alpha survives several collisions intact, its energy eventually becomes less than the Coulomb barrier. After some time, breakup occurs and the resultant excited system will undergo evaporation. This process is labeled CN; however, compound nucleus production also includes those events in which the alpha breaks up during the preequilibrium phase, after, for example, one collision, if no one of the resultant nucleons is subsequently emitted before equilibration. Obviously the probability of formation of the compound nucleus decreases with increasing incident energy owing to the increased probability of emission of one or more fast preequilibrium particles. While most of the preequilibrium yield of alphas is due to the mechanism α,α' above, some alphas are emitted as a result of the interaction of preequilibrium nucleons with preformed alpha clusters in the target nucleus.

The most likely single process at all energies is the breakup of the alpha particle following a single collision. This process increases with increasing energy owing to the increasing cross section for inelastic scattering between an alpha and a free nucleon with increasing center-of-mass energy. (Sec. III E.) The relative constancy of breakup following 2—5 collisions is fortuitous. The probability of multiple collisions occurring increases with energy, but the probability of alpha breakup after several collisions is small, owing to a decreasing inelastic scattering cross section. The two trends tend to cancel out.

Overall, breakup processes are seen to dominate events initiated by an alpha-nucleon collision, accounting for 60—70% of σ_R^α. Since a substantial amount of the remainder of the total reaction cross section comes from dissolution of the alpha to four nucleons in the nuclear field, spallation events are seen to arise predominantly from mechanisms in which the alpha particle breaks into its constituent nucleons, initiating a preequilibrium cascade.

a. $^{93}Nb(\alpha,xn)^{97-x}$ Tc reactions (Figs. 5—8). The excitation functions for the ^{93}Nb(α,1—5n) reactions are compared with the calculated results of the OMEGA calculation in Figs. 5—8. The (α,n) excitation function at energies above 30 MeV is almost entirely (>90%) due to events in which the alpha particle dissolves to four nucleons in the nuclear field with subsequent emission of a single fast neutron. This reaction may be considered the neutron equivalent to the events defining the high energy region of the proton spectrum described above; taken together, they provide justification of the mechanistic assumption and the equiprobability hypothesis of energy partition. Other mechanisms considered here fail to reproduce the slope of the experimental data. Breakup of the alpha following collision with a nucleon produces a division of the incident alpha energy among too many excitons. Emission of a single fast neutron with no subsequent evaporation is much less probable than that experimentally observed. An increasingly significant fraction of reactions leading to 2—5 neutron emission comes from breakup following one or more collisions; for example, the peak region in the (α,5n) reaction results from roughly equal contributions (15±10 mb) from six reaction paths: compound nucleus, dissolution in the nuclear field, and

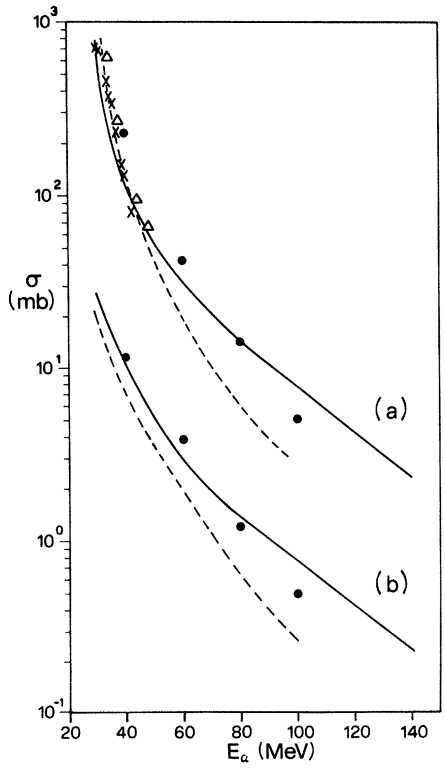

FIG. 5. Comparison of experimental and calculated excitation functions for the reactions ^{93}Nb(α,n)^{96}Tc, (b), and ^{93}Nb(α,2n)^{95}Tc, (a). Here and in most of the following figures, the ● represent the experimental cross sections from this work and the dashed line is a smooth line through the data of Ref. 18. The solid line is the result of the calculation. Other experimental values are from Ref. 37, ×, and Ref. 38, △.

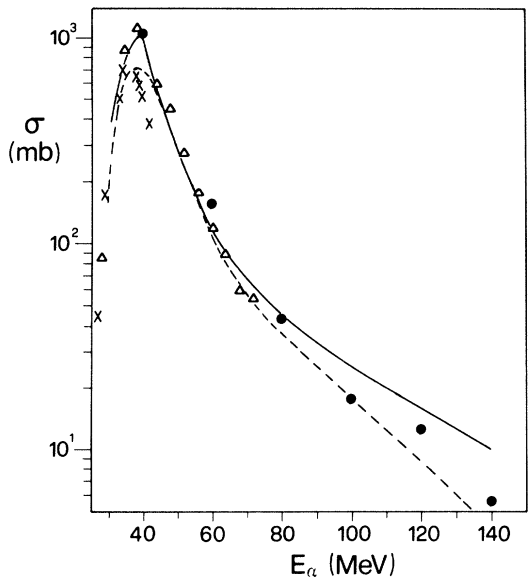

FIG. 6. Comparison of experimental and calculated excitation functions for the reaction ^{96}Nb(α,3n)^{94}Tc. The experimental data are from Ref. 18, dashed line; Ref. 37, ×; Ref. (38), △; and this work, ●. The results of the calculation are represented by the full line.

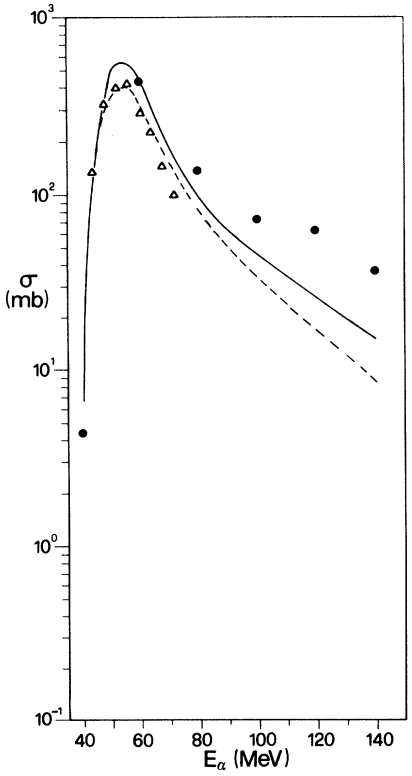

FIG. 7. Comparison of experimental and calculated excitation functions for the reaction ^{93}Nb(α,4n)^{93}Tc. The experimental data are from Ref. 18, dashed line; Ref. 38, △; and this work, ●. The results of the calculation are represented by the full line.

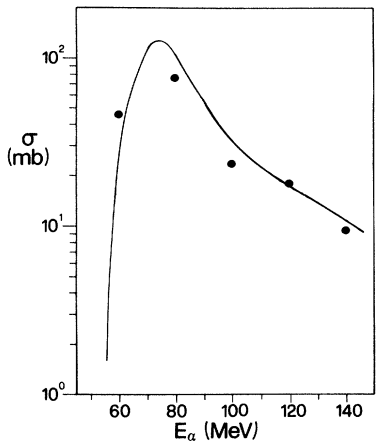

FIG. 8. Comparison of experimental and calculated excitation functions for the reaction ^{93}Nb(α,5n)^{92}Tc. The experimental data are from this work, ●. The results of the calculation are represented by the full line.

breakup following one, two, three, or four collisions.

Agreement between experimental data and the OMEGA calculation (the full line in all the figures) is quite good for all (α,xn) reactions, the only discrepancy appearing with the (α,4n) experimental data measured in this work. In this case, the calculation agrees reasonably well with the data measured by Ernst and co-workers.[18] The origin of the discrepancy between the two sets of data is not clear.

b. ^{93}Nb(α,p6n)^{90}Mo and ^{93}Nb(α,2p)^{95}Nb reactions (Fig. 9). The calculated values of the cross section for the (α,p6n) reaction underestimate the yields measured in this work by about 30% while agreeing with those of Ernst[18] at the higher incident energies. Most of the yield comes from evaporation with, at most, the emission of one preequilibrium particle at higher energies. Taken together with the generally good reproduction of the excitation functions for the (α,xn) reactions, this suggests that the evaluation of the probability of compound nuclear and simple one particle out preequilibrium events by the model is quite successful.

The absolute values of the cross sections for the (α,2p) reaction peak at 1—2 mb decreasing to about 0.5 mb at the highest energy. Thus these events occur with a probability of about one in two thousand. Given the random statistical nature of the calculation the agreement between theory and experiment is not unreasonable.

The mechanism is almost entirely the preequilibrium emission of two protons. A detailed analysis of the OMEGA results shows roughly equal contribution from four-particle dissolution in the nuclear field and breakup following the first collision with a nucleon; no other mechanism accounts for more than 1—2 % of the yield at any energy. In both cases, essentially all of the energy of the incident alpha is removed by emission of two fast protons; there is little or no contribution from evaporation.

c. ^{93}Nb(α,2pxn)$^{97-x}$Nb reactions (Figs. 10 and 11). From the mechanistic point of view, some of the most interesting results of the OMEGA calculation are for the (α,2pxn) reactions, a major component of which is the

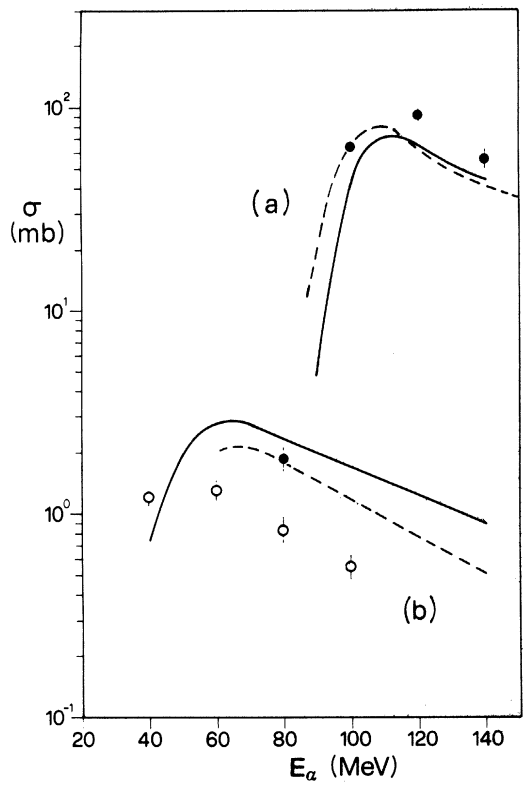

FIG. 9. Comparison of experimental and calculated excitation functions for the reactions ^{93}Nb(α,p6n)^{90}Mo, (a), and ^{93}Nb(α,2p)^{95}Nb, (b). The experimental data are from this work, filled and open dots, and Ref. 18, dashed line. The results of the theoretical calculations are the full lines.

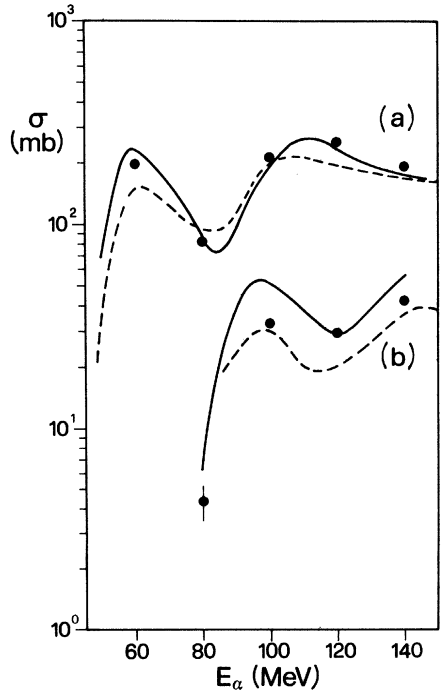

FIG. 10. Comparison of experimental and calculated excitation functions for the reactions ^{93}Nb(α,2p5n)^{90}Nb, (a), and ^{93}Nb(α,2p7n)^{88}Nb, (b). The experimental data are from Ref. 18, dashed lines, and this work, ●. The results of the calculations are represented by the full lines.

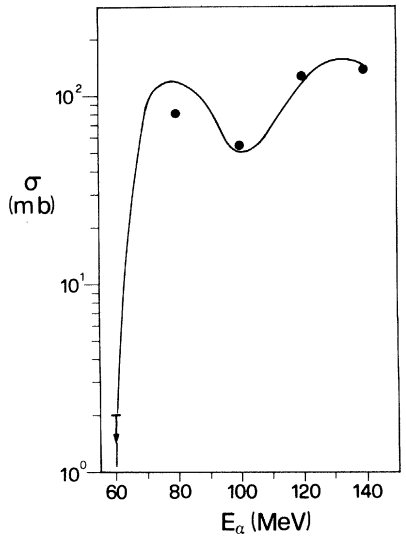

FIG. 11. Comparison of experimental and calculated excitation functions for the reaction ^{93}Nb(α,2p6n)^{89}Nb. The experimental data are from this work, ●. The results of the calculation are represented by the full line.

(α,αx −2n) reaction. The first peak arising mainly from evaporation of alphas is somewhat overestimated, the second coming from long evaporation chains including emission of two protons is reproduced satisfactorily.

Because of the complexity of these reactions, it is worth taking the particular case of the (α,2p5n) reaction, and considering its component parts in some detail. (See Fig. 10.) In the first peak (energetic considerations require emission of an alpha particle), less than 20% of the cross section results from events in which the incident alpha is reemitted. About 75% comes from production of a compound nucleus with evaporation of an alpha and three neutrons, the remainder being accounted for by preequilibrium processes emitting a nucleon. Most of these compound nucleus reactions originate in events in which the incident alpha particle disintegrates either in the nuclear field or following one or more collisions with nucleons.

At the energy of the first peak ($\sim$60 MeV), preequilibrium emission of a fast neutron virtually eliminates, for energetic reasons, the possibility of evaporation of sufficient further particles to produce the (α,α3n) product. Turning to the second peak around 110 MeV in the same reaction, the OMEGA calculation suggests different mechanisms of production.

Reemission of the incident alpha continues to account for slightly less than 20% of the reaction cross section. Evaporation of individual nucleons from a compound nucleus formed either following alpha particle dissolution in the nuclear field or in alpha-nucleon collisions is the main contribution. After the second maximum, the contribution from processes in which a preequilibrium nucleon is emitted increases with energy.

In this reaction, as well as in the other (α,2xpn) reactions, the contribution of interactions in which the incident alpha particle is reemitted is approximately independent of energy: the cross section corresponding to

this process is $\sim 40 \pm 10$ mb in the case of the (α,2p5n) reaction from 55 to 140 MeV, $\sim 20 \pm 10$ mb in the case of the (α,2p6n) reaction from 70 to 140 MeV, and $\sim 10 \pm 3$ mb from 90 to 140 MeV in the case of the (α,2p7n) reaction.

Thus in the valley between the two peaks, $\sim 50\%$ of the total yield in the case of (α,2p5n) and (α,2p6n) reactions and 30% in the case of the (α,2p7n) reaction comes from preequilibrium reemission of the incident alpha particle. It reflects the probability of alpha-nucleon collisions with transfer of some tens of MeV to the nucleus and reemission of the alpha. In turn, this arises from the kinematics of alpha scattering with free nucleons used to determine the nuclear configuration after scatter. (See Sec. III E.) Thus, in neither the first nor the second peak of these excitation functions is the preequilibrium emission of the incident alpha particle the dominant mechanism. However, it is the principal mechanism at intermediate energies where formation of a compound nucleus leads to evaporation of too many particles, but emission of a fast preequilibrium nucleon results in too few particles being evaporated.

d. $^{93}Nb(\alpha,3pxn)^{94-x}Zr$ *reactions (Figs. 12–14).* In Figs. 12–14 the excitation functions calculated for (α,3p5–8n) reactions are compared with experiment. The predominant mechanism in the region of the first peak of the excitation function, and in the region following the valley after the first peak, is evaporation from a compound nucleus. In most cases this compound nucleus is formed following the breakup of the alpha in a collision with a nucleon. The first peak, well reproduced by the OMEGA calculation, requires evaporation of both a proton and an alpha.

As discussed above, the calculated contribution from processes in which a fast alpha is emitted in the preequilibrium phase is rather independent of the incident alpha energy for all of these reactions. It amounts to 20–30 % of the total cross section.

e. $^{93}Nb(\alpha,4pxn)^{93-x}Y$ *reactions (Figs. 15–17).* Because of the energetics of these reactions, the first peak of the experimental data corresponds almost entirely to (α,2αx –4n) reactions, and as far as may be observed, the second peak to (α,α2px –2n) reactions. Of great interest is the contribution of preequilibrium alpha emission to these reactions. Even in the first peak, a notable contribution [as great as 50% of the total cross section in the case of the (α,4p5n) reaction] arises from these events. The reaction path including the preequilibrium emission of an alpha is dominant (85–90 %) in the valley for all four reactions, and amounts to $\sim 30\%$ in the second peak region.

Unlike reactions discussed previously, the second peak in these reactions differs greatly in magnitude from the first peak, greatly increasing when the emission of sufficient individual nucleons becomes energetically possible.

Thus it is interesting that the one-alpha-out reactions, which might be expected to be greatly enhanced by the possibility of reemission of the incident alpha seem, in fact, to stem mainly from pure evaporation. On the other hand, two alpha emission requires a substantial contribution from preequilibrium emission.

f. Other reactions, $^{93}Nb(\alpha,xpyn)$, $x \geq 5$, $y \geq 7$ *(Figs. 18*

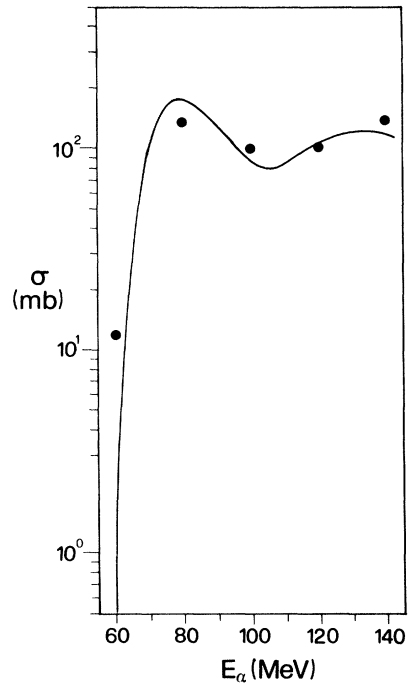

FIG. 12. Comparison of experimental and calculated excitation functions for the reaction ^{93}Nb(α,3p5n)^{89}Zr. The experimental data are from this work, ●. The results of the theoretical calculation are represented by the full line.

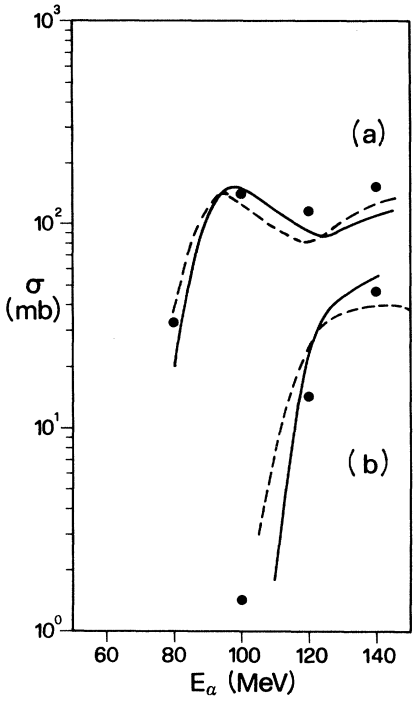

FIG. 13. Comparison of experimental and calculated excitation functions for the reactions ^{93}Nb(α,3p6n)^{88}Zr, (a), and ^{93}Nb(α,3p8n)^{86}Zr, (b). The experimental data are from Ref. 18, dashed lines, and this work, ●. The results of the calculation are represented by the full line.

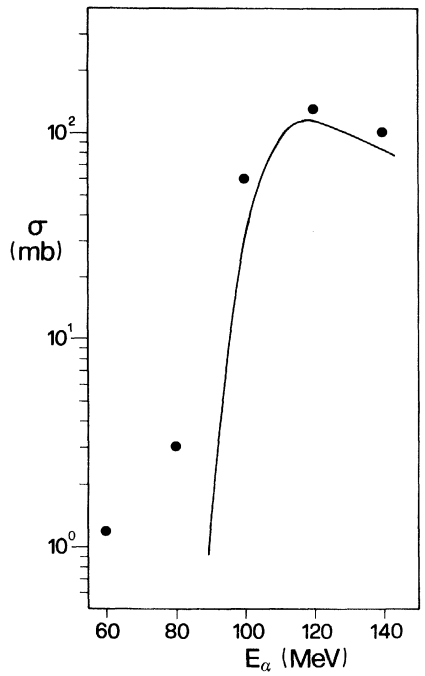

FIG. 14. Comparison of experimental and calculated excitation functions for the reaction ^{93}Nb(α,3p7n)^{87}Zr. The experimental data are from this work, ●. The results of the calculation are represented by the full line. The measured cross sections below 80 MeV, at least in part, are due to reaction paths that, in order to reduce the computing time, have been neglected in this calculation. The most energetically favored reaction path below 80 MeV is (α,αt3n), where all emitted particles are evaporated by compound nucleus. We restricted the evaporation to n, p, and α's.

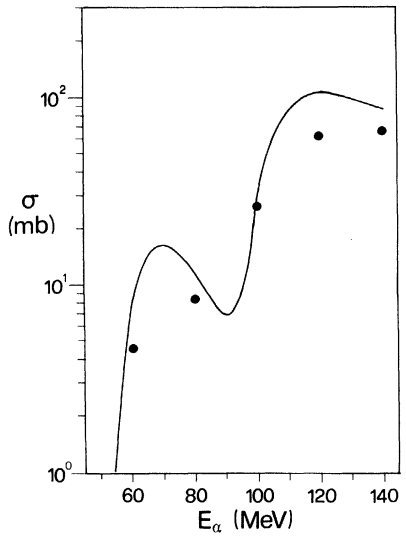

FIG. 16. Comparison of experimental and calculated excitation functions of the reactions ^{93}Nb(α,4p6n)^{87}Y. The experimental data are from this work, ●. The results of the calculation are represented by the full line.

and 19). Scattered experimental data exist for reactions in which two alphas, at least one proton, and several neutrons are emitted. In general, experimental cross sections range from 0.1 to 10 mb. Agreement between the theory and experiment is quite reasonable although there is considerable statistical uncertainty in the calculated results (as much as 100% and 50% for, respectively, 0.1 mb and 1.0

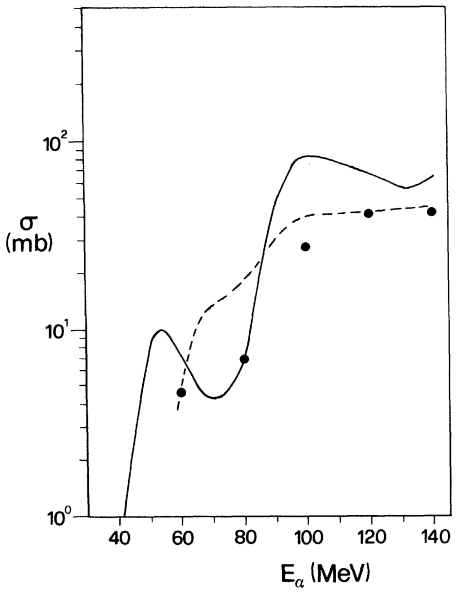

FIG. 15. Comparison of experimental and calculated excitation functions of the reaction ^{93}Nb(α,4p5n)^{88}Y. The experimental data are from Ref. 18, dashed line, and this work, ●. The results of the calculation are represented by the full line.

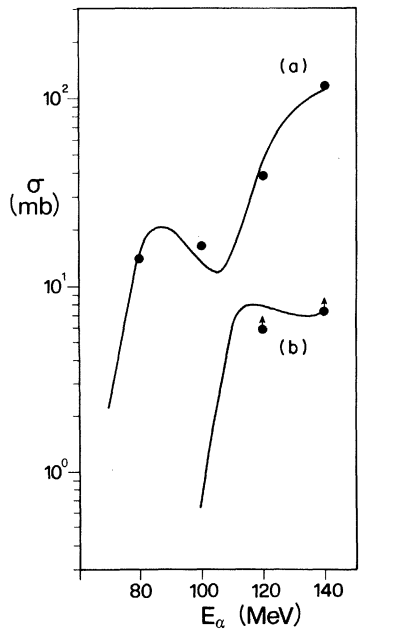

FIG. 17. Comparison of experimental and calculated excitation functions of the reactions ^{93}Nb(α,4p7n)^{86}Y, (a), and ^{93}Nb(α,4p9n)^{84}Y, (b). The experimental data are from this work, ●. The results of the calculation are represented by the full lines.

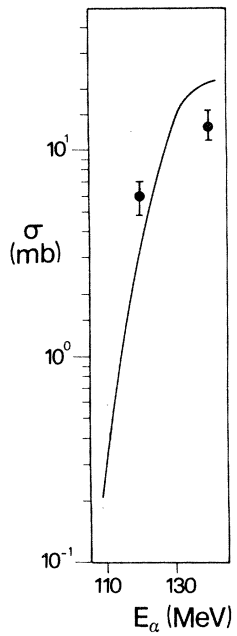

FIG. 18. Comparison of experimental and calculated excitation functions of the reaction ^{93}Nb(α,5p9n)^{83}Sr. The experimental data are from this work, ●. The results of the calculation are represented by the full line.

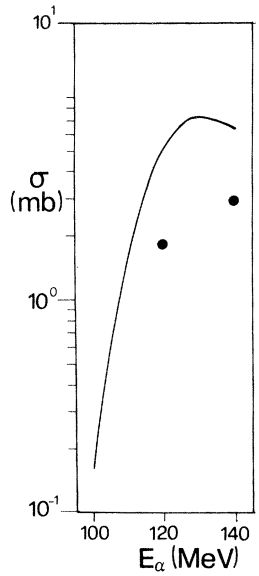

FIG. 19. Comparison of experimental and calculated excitation functions of the reaction ^{93}Nb(α,6p7n)^{84}Rb. The experimental data are from this work, ●. The results of the calculation are represented by the full line.

mb cross sections). The calculation tends to overestimate the yield of two and three alpha emission reactions.

C. Summary of the results of the OMEGA model

The purpose of this work was to present a comprehensive model of the interaction of an incident alpha particle with a complex nucleus, and use it to reproduce both charged particle spectra and a wide range of excitation functions. Apart from a small systematic overestimate of alpha particle emission in the *evaporation* phase of the model, the OMEGA calculation has produced very satisfactory results. With no freely varying parameters, excitation functions for reactions proceeding largely by direct interaction, by compound nucleus formation, by multiple scattering, and by breakup processes, were all reproduced, along with both alpha particle and proton spectra at both low and high incident energies.

When comparing results of alpha induced reactions with different models, it must be stressed that comparison to a reduced set of experimental data may not be sufficient to obtain meaningful information on the reaction mechanism. For example, the contribution of preequilibrium emission of alpha particles to (α,2pxn) reactions is quite small, and could be greatly underestimated without seriously affecting the fit to the experimental data, especially in the peak regions of the excitation functions. In addition, since reactions in which several particles are emitted mainly proceed through evaporation from a compound nucleus, they are rather insensitive to the mode of interaction of the alpha and nucleus, provided that a sufficiently large initial exciton number be employed for evaluating the intranuclear cascade of nucleon-nucleon collisions through which the composite system deexcites.

ACKNOWLEDGMENTS

Experiments were performed by J.J.H. while a vistor at the University of Maryland Cyclotron, and by B.V.J. and J.J.H. at the University of California, Lawrence Berkeley Laboratory. We gratefully acknowledge the encouragement, support, and facilities of Professors W. B. Walters (Maryland) and G. T. Seaborg (Berkeley). We are pleased to acknowledge discussions with Professor H. D. Holmgren of the University of Maryland, whose experimental data provide much of the basis for the model presented, and with Prof. P. E. Hodgson. This work was made possible by support from the Natural Sciences and Engineering Research Council of Canada, the National Institute of Nuclear Physics, Milan, Italy, the Italian Ministry of Public Instruction, and the United States Department of Energy.

---

*Present address: Cyclotron Laboratory, Michigan State University, East Lansing, MI 48823.

[1]M. Blann, Annu. Rev. Nucl. Sci. 25, 123 (1975), and references therein.

[2]E. Gadioli, Nukleonika 21, 385 (1976), and references therein.

[3]E. Gadioli, E. Gadioli-Erba, and J. J. Hogan, Phys. Rev. C 16, 1404 (1977).

[4]E. Gadioli, E. Gadioli-Erba, and J. J. Hogan, Nuovo Cimento

40A, 383 (1977).
[5]J. J. Hogan, E. Gadioli, E. Gadioli-Erba, and C. C. Chung, Phys. Rev. C 20, 1831 (1979).
[6]E. Gadioli, E. Gadioli-Erba, J. J. Hogan, and K. I. Burns, Z. Phys. A 301, 289 (1981).
[7]R. Michel and G. Brinkmann, Nucl. Phys. A338, 167 (1980).
[8]P. W. Gallagher, Ph.D. thesis, University of Maryland, 1980 (unpublished); P. W. Gallagher, W. B. Walters, and C. Chung, in *Proceedings of the 3rd International Conference on Nuclear Reaction Mechanisms, Varenna, 1982,* edited by E. Gadioli (University of Milano, Milano, 1982).
[9]R. Ibowski, W. Scholz, J. Bisplinghoff, J. Ernst, H. Keuser, T. Mayer-Kuckuk, and H. Machner, in *Proceedings of the 2nd International Conference on Nuclear Reaction Mechanisms, Varenna, 1979* (University of Milano, Milano, 1979).
[10]A. Mignerey, M. Blann, and W. Scobel, Nucl. Phys. A273, 125 (1976).
[11]J. R. Wu and C. C. Chang, Phys. Rev. C 16, 1812 (1977); 17, 1540 (1978).
[12]R. W. Koontz, C. C. Chang, H. D. Holmgren, and J. R. Wu, Phys. Rev. Lett. 43, 1862 (1979).
[13]H. J. Probst, S. M. Qaim, and R. Weinreich, Int. J. Appl. Radiat. Isot. 27, 431 (1976).
[14]C. Williamson and J. P. Boujot, Commissariat á l'Energie Atomique Report CEA 2189, 1962.
[15]*Table of Isotopes, 7th ed.,* edited by C. M. Lederer and V. S. Shirley (Wiley, New York, 1977).
[16]A preliminary set of data appeared (Ref. 17) several years ago in an annual report of the Lawrence Berkeley Laboratory. The present data in final form reflects further analysis of complex decay curves, more recent decay scheme studies, and the correction of several inadvertent typographical errors.
[17]J. J. Hogan and B. V. Jacak, Lawrence Berkeley Laboratory Report LBL 9711, 1979.
[18]H. Stockhorst, W. Friedland, and J. Ernst, in *Proceedings of the 3rd International Conference on Nuclear Reaction Mechanisms, Varenna, 1982,* edited by E. Gadioli (University of Milano, Milano, 1982).
[19]In comparing our data with those of Ernst *et al.,* one has to consider two characteristics of stacked foil experiments: first, the spread in beam energy, and second, the effect of secondary particle interactions. In most of the experiments done by the Ernst group, the incident beam energy was degraded by 80—110 MeV. While the average beam energy passing through a foil was calculated from the same range-energy tabulations of Williamson and Boujot (Ref. 14) used in this work, the spread in beam energies about the average is considerable after passage through as much as 1000 mg/cm^2 of target. This affects excitation functions in their strongly energy dependent regions in an unpredictable fashion due to the unknown energy distribution of incident particles striking a given foil. Secondly, as shown by Holmgren *et al.* (Ref. 20), alpha interactions with heavy nuclei produce a strongly forward peaked flux of fast p, d, t, and ^{3}He. It is unclear how strongly these may affect the spallation yields, but like the first effect, it *is* clear that the effect becomes larger in traversing the thickly stacked foils. Nevertheless, such experiments are highly valuable in that they produce much more complex excitation functions than those measured from individual experiments.
[20]J. R. Wu, C. C. Chang, H. D. Holmgren, and R. W. Koontz, Phys. Rev. C 20, 1284 (1979).
[21]C. Mayer-Böricke, Nukleonika 22, 1131 (1977).
[22]G. Chevenert, N. S. Chant, I. Halpern, G. Glashausser, and D. L. Hendrie, Phys. Rev. Lett. 27, 434 (1971).
[23]H. D. Holmgren, C. C. Chang, R. W. Koontz, and J. R. Wu, *Proceedings of the 2nd International Conference on Nuclear Reaction Mechanisms, Varenna, 1979* (University of Milano, Milano, 1979).
[24]E. Gadioli and E. Gadioli-Erba, Z. Phys. A 299, 1 (1981).
[25]D. R. Brown, I. Halpern, J. R. Calarco, P. A. Russo, D. L. Hendrie, and H. Homeyer, Phys. Rev. C 14, 896 (1976).
[26]J. R. Wu, C. C. Chang, and H. D. Holmgren, Phys. Rev. C 19, 659 (1979).
[27]R. W. West, Phys. Rev. 141, 1033 (1966).
[28]N. Chevarier, Ph.D. thesis, Université C. Barnard, Lyon, France, 1973 (unpublished); A. Chevarier, N. Chevarier, A. Demeyer, G. Hollinger, P. Pertosa, and Tran Minh Duc, Phys. Rev. C 8, 2155 (1973).
[29]L. W. Put and A. M. J. Paans, Phys. Lett. B49, 266 (1974).
[30]P. Schwandt and P. P. Singh, Nukleonika 21, 451 (1976).
[31]A. Ferrero, E. Gadioli, E. Gadiloli-Erba, I. Iori, N. Molho, and L. Zetta, Z. Phys. A 293, 123 (1979).
[32]E. Gadioli, E. Gadioli-Erba, I. Iori, and L. Zetta. J. Phys. G 6, 1391 (1980).
[33]A. Budzanowski, G. Baur, C. Alderliestein, J. Bojowald, C. Mayer-Böricke, W. Oelert, P. Turek, F. Rosel, D. Trautmann, Phys. Rev. Lett. 41, 635 (1978).
[34]A. Budzanowski, G. Baur, R. Shyam, J. Bojowald, W. Oelert, G. Reipe, M. Rogge, P. Turek, F. Rosel, and D. Trautmann, Z. Phys. A 293, 293 (1979).
[35]G. Baur, R. Shyam, F. Rosel, and D. Trautmann, Helv. Phys. Acta 53, 506 (1980).
[36]G. Baur, R. Shyam, F. Rosel, and D. Trautmann, Phys. Rev. C 21, 2668 (1980).
[37]T. Matsuo, J. M. Matuszek, N. D. Dudey, and T. T. Sugihara, Phys. Rev. 139, B886 (1965).
[38]C. L. Branquinho, S. M. A. Hoffmann, G. W. A. Newton, V. J. Robinson, H. Y. Wang, I. S. Grant, and J. A. B. Goodall, J. Inorg. Nucl. Chem. 41, 617 (1979).
[39]At 140 MeV with a Zr target, the mean angular momentum deposited by alpha particles dissolving in the nuclear field or breaking up following collision with a nucleon is evaluated to be $\sim 26\hbar$. The first preequilibrium proton, assumed to be aligned with the incident alpha particle direction, on the average, carries away $\sim 6.5\hbar$ thus leaving a residual system with a average angular momentum $J \sim 19.5\hbar$, parallel to $\vec{1}_\alpha$. Also a second chance preequilibrium fast particle will tend to be emitted preferentially aligned with the alpha; however, subsequent evaporated particles are emitted more or less isotropically and affect the average angular momentum of the residual nucleus very little. This situation remains until the excitation energy is small and effects arising from population of the yrast levels must be considered. The last evaporated particle (consideration of neutron and proton separation energies suggest proton emission is a non-negligible component) will carry away a small energy and, as a consequence, a small as possible angular momentum. Since the residual nucleus at the end of the evaporation chain is left with a quite small excitation energy, its angular momentum cannot exceed a J_R which is expected to be notably smaller than the angular momentum of the decaying parent nucleus. Then, the last evaporated particle, to fulfill the conservation of total angular momentum, will be forced to have an l parallel to $\vec{1}_\alpha$.